



**C–H Amination Chemistry Mediated by Trinuclear Cu(I)
Sites Supported by a Ligand Scaffold Featuring an Arene
Platform and TetramethylguanidinyI Residues†**

Journal:	<i>Dalton Transactions</i>
Manuscript ID	DT-ART-06-2024-001670.R1
Article Type:	Paper
Date Submitted by the Author:	22-Aug-2024
Complete List of Authors:	Sharma, Meenakshi; Missouri University of Science and Technology, Chemistry Fritz, Reece M.; Missouri University of Science and Technology, Department of Chemistry Bhatia, Himanshu; Missouri University of Science and Technology, Department of Chemistry Adebanjo, Joseph; University of North Texas, Chemistry Lu, Zhou; University of North Texas, Department of Chemistry Omary, Mohammad; University of North Texas, Chemistry Cundari, Thomas; University of North Texas, Chemistry Choudhury, Amitava; Missouri University of Science and Technology, Chemistry Stavropoulos, Pericles; Missouri University of Science and Technology, Department of Chemistry

**C–H Amination Chemistry Mediated by Trinuclear Cu(I) Sites
Supported by a Ligand Scaffold Featuring an Arene Platform and
Tetramethylguanidinyll Residues[†]**

Meenakshi Sharma,^a Reece M. Fritz,^a Himanshu Bhatia,^a Joseph O. Adebajo,^b Zhou Lu,^{b,c}
Mohammad A. Omary,^b Thomas R. Cundari,^{b,*} Amitava Choudhury,^a and Pericles Stavropoulos^{a,*}

^a Department of Chemistry, Missouri University of Science and Technology, Rolla, MO 65409, USA.

^b Department of Chemistry, University of North Texas, Denton, TX 76203, USA.

^c Present address: Department of Chemistry, University of Rochester, Rochester, NY 14627, USA.

* To whom correspondence should be addressed. Tel.: (+1) 573-341-7220, Fax: (+1) 573-341-6033. E-mail: pericles@mst.edu

[†]Electronic Supplementary Information (ESI) available: synthetic protocols, NMR spectra, X-ray crystallography data, computational xyz files and additional computational details, figures and tables as noted in the text. See DOI: 10.1039/xxxx

Abstract: Tripodal ligands that can encapsulate single or multiple metal sites in C_3 -symmetric geometric configurations constitute valuable targets for novel catalysts. Of particular interest in ligand development are efforts toward incorporating apical elements that exhibit little if any electron donicity, to enhance the electrophilic nature of a trans positioned active oxidant (e.g., metal-oxo, -nitrene). The tripodal ligand TMG₃trphen-Arene has been synthesized, featuring an arene platform 1,3,5-substituted with phenylene arms possessing tetramethylguanidiny (TMG) residues. Compound [(TMG₃trphen-Arene)Cu₃(μ-Cl)₃] has been subsequently synthesized by extracting a Cu₃(μ-Cl)₃ cluster from anhydrous CuCl and shown to encapsulate a crown-shaped Cu₃(μ-Cl)₃ fragment, supported by Cu–N_{TMG} bonds and modest Cu₃⋯arene long-range contacts. Energy decomposition analysis (EDA) indicates that electrostatic contributions to the total interaction energy far exceed those due to orbital interactions. The latter involve orbital pairings largely associated with the N_{TMG} stabilization of the Cu₃(μ-Cl)₃ cluster. The independent gradient model based on the Hirshfeld partition (IGMH) corroborates that contacts between the arene platform and the Cu₃ triangle are noncovalent in nature. Catalyst [(TMG₃trphen-Arene)Cu₃(μ-Cl)₃] enables amination of sec-benzylic and tert-C–H bonds of a panel of substrates by pre-synthesized PhINTces in solvent matrices that incorporate small amounts of HFIP. The involvement of an electrophilic aminating agent is evidenced by the better yields obtained for electron-rich benzylic sites and is further supported by Hammett analysis that reveals the development of a small positive charge during C–H bond activation. A rather modest KIE effect (2.1) is obtained from intramolecular H(D) competition in the amination of ethylbenzene, at the borderline of reported values for concerted and stepwise C–H amination systems. DFT analysis of the putative copper-nitrene oxidant indicates that the nitrene N atom is bridging between two

copper sites in closely spaced triplet (ground state) and broken-symmetry singlet electronic configurations.

Introduction

Amines constitute a class of compounds that finds extensive applications in several chemical industries, such as in the production of pharmaceuticals, agrochemicals, dyes, plastics, semiconductors, solvents and many other materials essential to societal needs.¹ The construction of a key C–N bond can be achieved by cross-coupling methodologies requiring an energetic C–X precursor (X = halide, pseudohalide, boronic acids, stannanes, siloxanes) to influence reactivity and guide selectivity.² An alternative, potentially more atom- and energy-economical approach involves activated or non-activated C–H/C=C feedstock, to which a nitrene/nitrenoid can insert with the assistance of metal-catalyzed or organocatalytic methodologies.³ Naturally, the issue of C–H bond reactivity/selectivity and mode of nitrene/nitrenoid insertion become more challenging in these approaches,⁴ hence the science of catalyst development plays a crucial role in enabling pathways that, on occasion, could even circumvent substrate predilections.⁵

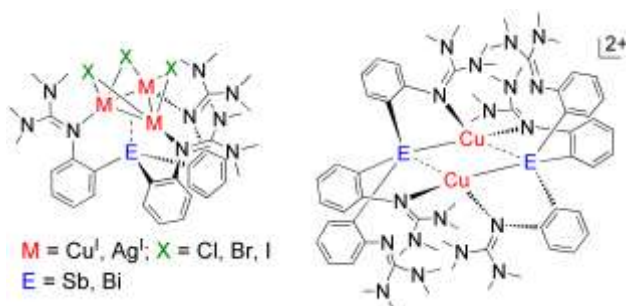
Figure 1. Catalysts supported by axial N_{amine} coordination and TMG residues



Recent work in our laboratories has emphasized the use of superbasic tetramethylguanidiny (TMG) residues⁶ in stabilizing tripodal N₃N (TMG₃trphen) and bipodal N₂N (TMG₂biphen) ligand scaffolds that are analogs of the TMG₃tren and TMG₂dien ligand frameworks,⁷ respectively (Figure 1). The phenylene linkers tend to provide more rigidity and stability (lack of β -hydride cleavage pathways), as well as a weaker equatorial ligand field, resulting in metal reagents that are on average more reactive in nitrene-transfer chemistry. Indeed, monocationic Cu(I) catalysts have been employed in C–H aminations and amidinations (in the presence of nitriles),⁸ whereas dicationic base-metal congeners (M = Mn^{II}, Fe^{II}, Co^{II}) have found use in the synthesis of three- and five-membered *N*-heterocycles from C=C feedstocks.⁹

Whereas in all cases noted above the axial coordination is occupied by a hard donor (N_{amine}), more recent efforts have been targeting weaker electron donors in the apical position, such as the heavier pnictogens Sb(III) and Bi(III), in attempts to increase the electrophilicity of any trans-positioned metal nitrene.¹⁰ However, these elements enlarge the ligand cavity significantly, and facilitate the synthesis of polynuclear species [(TMG₃trphen-E)Cu₃(μ -X)₃] and [(TMG₃trphen-E)₂Cu₂](PF₆)₂ (E = Sb, Bi) from CuX (X = Cl, Br, I) and [Cu(NCMe)₄](PF₆), respectively (Figure 2).¹¹ These species are capable of mediating C–H aminations (especially for benzylic substrates) and C=C aziridinations, but are less reactive than the mononuclear N_{amine}-supported Cu(I) sites.

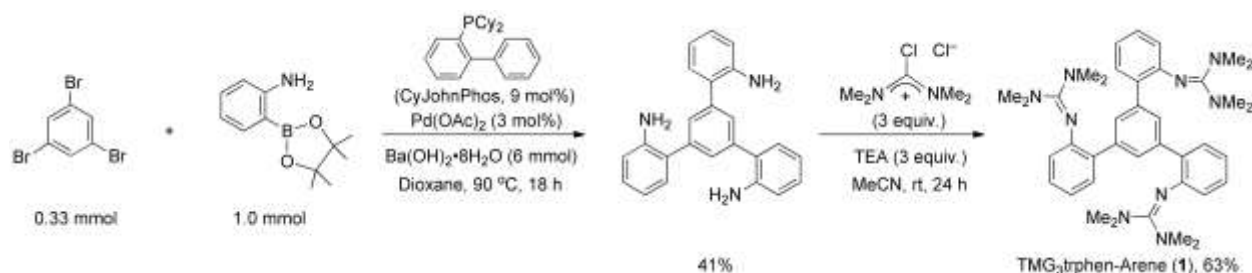
Figure 2. Reagents supported by heavier pnictogens (Sb, Bi) and TMG residues



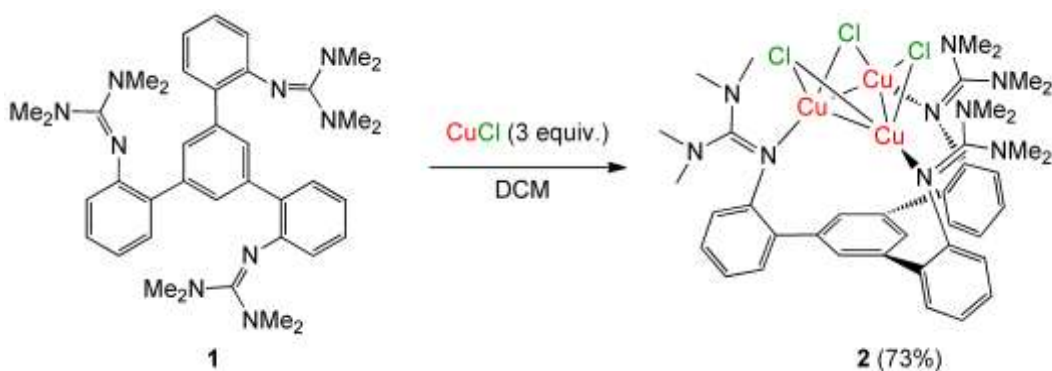
In the present manuscript, we are exploring the limits of the ligand cavity enlargement by selecting an arene plane, in lieu of a pnictogen element, to occupy the apical position and further weaken the electron-donicity offered by ligand residues along the axial dimension. Arene platforms have attracted special attention in ligand construction methodologies.¹² Given their ability to capture both single and multiple-metal sites and assemblies, they provide an opportunity to study metal isolation and/or synergism in coordination and catalytic chemistry. We examine the nitrene-transfer chemistry mediated by a trinuclear copper(I) catalyst, encapsulated by an arene- and TMG-supported scaffold, and place its reactivity in a mechanistic context with the assistance of experimental and computational probes. As opposed to the N_{amine} -coordinated mononuclear Cu(I) sites that give rise to triplet $^3[\text{Cu}=\text{NR}]$ oxidants, the present systems are best understood by the action of bridging $\text{Cu}_2(\mu\text{-NR})$ units with closely spaced triplet (ground state) and singlet manifolds.

Results and Discussion

Synthesis of Ligand and Tricopper(I) Compound. The tripodal ligand $\text{TMG}_3\text{trphen-Arene}$ (**1**), featuring an 1,3,5-trisubstituted benzene platform and TMG arms (Scheme 1), is synthetically approached by first constructing the known trianiline¹³ via standard Pd-coupling of 1,3,5-tribromobenzene and 2-aminophenylboronic acid pinacol ester, followed by installation of the TMG groups with the assistance of chlorotetramethylformamidine chloride (prepared from tetramethylurea and oxalyl chloride).⁸ The ligand is obtained as colorless crystals from slowly crystallizing (initially oily) dichloromethane solutions. X-ray quality crystals can be obtained from layering pentane over dichloromethane solutions to afford $(\text{TMG}_3\text{trphen-Arene})\cdot 1.5\text{DCM}$.

Scheme 1. Synthesis of Ligand **1**

The reaction of ligand **1** with anhydrous CuCl (3 equiv.) in dichloromethane affords a yellow solution, from which light yellow-brown crystals of [(TMG₃trphen-Arene)Cu₃(μ-Cl)₃]·2.56CH₂Cl₂ (**2**) can be obtained upon layering with pentane (Scheme 2). Attempts to use 1 or 2 equiv. of CuCl still afford complex **2**, but in lower yields. By way of contrast, Itoh's TMG₃tach ligand, which features three TMG residues attached to a cyclohexane platform, has the capacity to capture only one Cu(II) site due to the narrower ligand cavity.¹⁴ Ligand **1** extracts a crown-shaped Cu₃(μ-Cl)₃ cluster in a similar manner to that noted above for the analogous Sb/Bi-containing ligands. Two other cases previously reporting Cu₃(μ-Cl)₃ extraction make use of triphosphino-stibene/bismuthine (o-(ⁱPr₂P)C₆H₄)₃E (E = Sb, Bi)¹⁵ and tris(2-(2-pyridyl)ethyl)phosphine ligands.¹⁶ Incidentally, the gas-phase structure of CuCl exhibits planar, *D*_{3h}-symmetric Cu₃Cl₃ rings (Cu–Cu = 2.627 ± 0.012, Cu–Cl = 2.166 ± 0.008 Å, Cu–Cl–Cu = 73.9 ± 0.6°, at 689 K).¹⁷

Scheme 2. Synthesis of Trinuclear Cu(I) Reagent [(TMG₃trphen-Arene)Cu₃(μ-Cl)₃] (**2**)

Solid-state Structures. Ligand TMG₃trphen-Arene (**1**) exhibits a solid-state conformation (Figure 3, Table S1) that is not unlike others that have been recently observed with Sb(III) and Bi(III) apical elements in lieu of the arene platform.^{11,18} An approximate C_3 axis relates the three TMG arms, which are positioned on the same side of the benzene ring, generating a well pre-organized cavity for metal complexation. By comparison to the analogous Sb/Bi-containing complexes, the cavity of **1** is significantly enlarged, as indicated by the average interatomic distances between the N(1)/N(4)/N(7) superbasic guanidinyll residues (6.403 ± 0.241 (**1**) vs 5.436 (Sb), 5.483 (Bi) Å)).

For compound **2** (Figure 4, Table S1), the unit cell is composed of two independent molecules, featuring left-hand (*M*) and right-hand (*P*) propeller conformations, associated with the 1,3,5-triarylbenzene blades.¹⁹ The Cu₃(μ-Cl)₃ unit is supported by three guanidinyll residues (Cu–N = 2.024 ± 0.007 (*M*), 2.022 ± 0.005 (*P*) Å) in a similar manner and almost identical strength to that encountered with the aforementioned [(TMG₃trphen-E)Cu₃(μ-Cl)₃] compounds (E = Sb, Bi),¹¹ despite the fact that the ligand cavity in **2** is considerably larger (N \cdots N = 6.200 ± 0.062 (*M*), 6.212 ± 0.046 (*P*) Å)). As a result, the crown-shaped Cu₃(μ-Cl)₃ unit exhibits longer Cu–Cu edges (Cu–Cu = 3.134 ± 0.064 (*M*), 3.174 ± 0.067 (*P*) Å), slightly shorter Cu–Cl bonds (Cu–Cl = 2.263 ± 0.011 (*M*), 2.264 ± 0.014 (*P*) Å) and wider Cu–Cl–Cu angles (Cu–Cl–Cu = 87.66 ± 1.96 (*M*), 89.02 ± 2.35 (*P*)°). The Cu–Cl bond distances reflect the degree of electron-donation of the apical element toward the Cu₃ triangle (Sb > Bi > Arene). Weak cuprophilic d¹⁰–d¹⁰ interactions are still possible in **2**, given the recently reassessed van-der-Waals radius of the Cu atom (≈ 1.96 Å),²⁰ even at distances more typical for intermolecular Cu^I \cdots Cu^I contacts ($2.6 - 3.6$ Å).²¹

The strong donicity of the TMG residues in **2** is depicted by the degree of charge delocalization within the CN₃ triangle, evaluated by the structural parameter $\rho = 2a/(b+c)$, where a is the C=N

bond distance and b and c are the two C–NMe₂ bond distances.²² For ligand **1** the length of the C=N bond is 94% of the average C–NMe₂ bonds ($\rho = 0.94$), whereas for complex **2** the three C–N bonds are almost equivalent ($\rho = 0.97$)

The Cu₃(μ -Cl)₃ cluster is located above the arene platform at a distance (C_{6,cent}–Cu_{3,cent} = 2.7054(2) (M), 2.7221(3) (P) Å) that rather precludes any strong Cu–arene interactions, although the distances between each Cu and two adjacent aromatic carbons (av. Cu(1)–C(5)/C(6) = 2.965 \pm 0.074, Cu(2)–C(3)/C(4) = 2.894 \pm 0.044, Cu(3)–C(1)/C(2) = 2.730 \pm 0.043 Å) can still signify weak Cu–arene contacts within the van-der-Waals limit (Cu–C = 3.10 Å). *Bona fide* Cu(I)- η^x -arene interactions ($x = 1 - 3, 6$) with ligand-untethered arenes are usually characterized by short Cu–C bond distances (2.06 – 2.48 Å),²³ but tethered versions can give rise to a wide range of Cu–C bonds or contacts (2.13 – 3.31 Å).²⁴ Long range Cu–arene interactions (2.7 – 3.2 Å) can also be found occasionally with solvated arene molecules.²⁵ Finally, the corresponding C–C bond distances of the coordinated arene in **2** (1.399 \pm 0.004 Å) are only slightly longer than those exhibited by the free arene in **1** (1.397 \pm 0.003 Å), adding another challenge in determining genuine Cu–C interactions at longer distances.

Solution Behavior. For [(TMG₃trphen-Arene)Cu₃(μ -Cl)₃] (**2**) only a single methyl peak of the TMG arm is observed by ¹H NMR at room temperature (δ (ppm, CD₂Cl₂, 298 K) = 2.78 (2.47, for ligand **1**). As opposed to the [(TMG₃trphen-E)Cu₃(μ -Cl)₃] compounds (E = Sb, Bi) that show broad TMG related peaks at room temperature,¹¹ the rotational restrictions for the TMG arms are significantly relaxed, by virtue of the more sizeable ligand cavity of **2**. The coordination of the superbasic N_{TMG} residues is also depicted by the downfield shift of the central CN₃ carbon atom in ¹³C NMR (166.6 ppm in **2** vs 158.3 ppm in **1**) and the equivalence of C–N₃ bond distances in **2** (SCXRD data). Otherwise, no significant NMR shifts are observed between **1** and **2** with regards

to the C, H atoms of the arene platform (for instance, the ^1H NMR peak for the arene C–H is at 7.50 ppm for **1** and **2**).

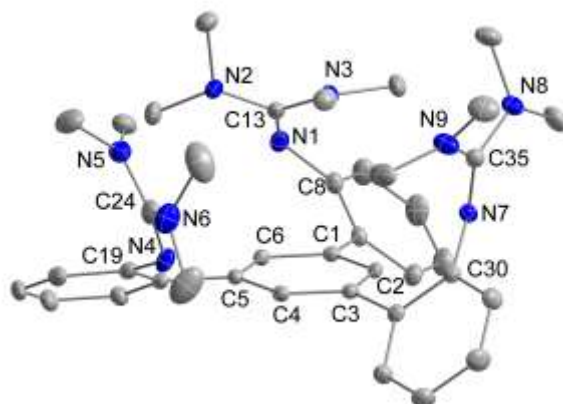


Figure 3. ORTEP Diagram (TMG₃trphen-Arene)•1.5CH₂Cl₂ (**1**) drawn with 40% thermal ellipsoids. Selective interatomic distances [Å] and angles [°] for **1**: N(1)–C(8) = 1.408(3), N(1)–C(13) = 1.293(3), N(2)–C(13) = 1.380(3), N(3)–C(13) = 1.373(3), N(4)–C(19) = 1.397(4), N(4)–C(24) = 1.292(4), N(5)–C(24) = 1.375(4), N(6)–C(24) = 1.383(4), N(7)–C(30) = 1.406(3), N(7)–C(35) = 1.289(3), N(8)–C(35) = 1.380(3), N(9)–C(35) = 1.383(3), C(8)–N(1)–C(13) = 122.2(2), N(1)–C(13)–N(2) = 119.0(2), N(1)–C(13)–N(3) = 126.5(2), N(2)–C(13)–N(3) = 114.5(2), C(19)–N(4)–C(24) = 121.2(2), N(4)–C(24)–N(5) = 126.6(3), N(4)–C(24)–N(6) = 118.9(3), N(5)–C(24)–N(6) = 114.5(3), C(30)–N(7)–C(35) = 120.3(2), N(7)–C(35)–N(8) = 119.8(2), N(7)–C(35)–N(9) = 126.6(2), N(8)–C(35)–N(9) = 113.6(2).

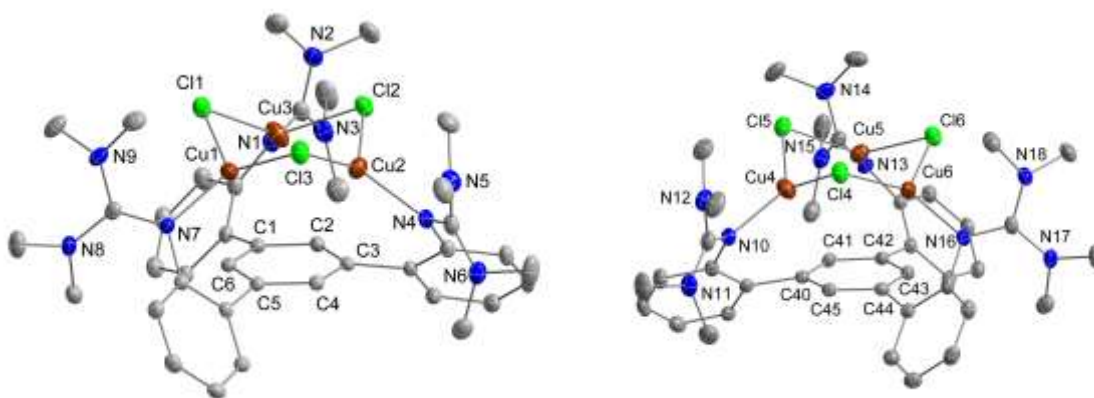


Figure 4. ORTEP diagram of [(TMG₃trphen-Arene)Cu₃(μ-Cl)₃]•2.56CH₂Cl₂ (left-hand (*M*), and right-hand (*P*) propeller) (**2**) drawn with 40% thermal ellipsoids. Selective interatomic distances

[Å] and angles [°]: Cu(1)–Cu(2) = 3.0532(7), Cu(1)–Cu(3) = 3.1411(10), Cu(2)–Cu(3) = 3.2085(10), Cu(1)–Cl(1) = 2.2766(10), Cu(1)–Cl(3) = 2.2449(11), Cu(1)–N(7) = 2.016(3), Cu(2)–Cl(2) = 2.2686(10), Cu(2)–Cl(3) = 2.2669(10), Cu(2)–N(4) = 2.023(3), Cu(3)–Cl(1) = 2.2509(11), Cu(3)–Cl(2) = 2.2703(10), Cu(3)–N(1) = 2.032(3), Cu(4)–Cu(5) = 3.097(7), Cu(4)–Cu(6) = 3.261(3), Cu(5)–Cu(6) = 3.163(2), Cu(4)–Cl(4) = 2.2834(11), Cu(4)–Cl(5) = 2.2544(11), Cu(4)–N(10) = 2.018(3), Cu(5)–Cl(5) = 2.2654(10), Cu(5)–Cl(6) = 2.2594(11), Cu(5)–N(13) = 2.028(3), Cu(6)–Cl(4) = 2.2432(11), Cu(6)–Cl(6) = 2.2776(11), Cu(6)–N(16) = 2.018(3), Cu(2)–Cu(1)–Cu(3) = 62.373(19), Cu(1)–Cu(2)–Cu(3) = 60.156(18), Cu(1)–Cu(3)–Cu(2) = 57.471(19), Cu(1)–Cl(1)–Cu(3) = 87.86(4), Cu(2)–Cl(2)–Cu(3) = 89.96(4), Cu(1)–Cl(3)–Cu(2) = 85.17(4), Cu(5)–Cu(4)–Cu(6) = 56.60(2), Cu(4)–Cu(5)–Cu(6) = 62.78(2), Cu(4)–Cu(6)–Cu(5) = 57.62(2), Cu(4)–Cl(4)–Cu(6) = 92.17(4), Cu(4)–Cl(5)–Cu(5) = 86.50(4), Cu(5)–Cl(6)–Cu(6) = 88.39(4).

Computational Studies. The structure of [(TMG₃trphen-Arene)Cu₃(μ-Cl)₃] (**2**) was optimized and found to agree with experimental data. The energy decomposition analysis (EDA)²⁶ decomposes the total interaction energy (ΔE_{int}) into four components: electrostatic attraction (ΔE_{elstat}), Pauli repulsion (ΔE_{Pauli}), orbital interaction (ΔE_{OrbInt}), and dispersion energy (ΔE_{disp}). The energetic pattern (Table 1) closely matches that previously observed for [(TMG₃trphen-E)Cu₃(μ-Cl)₃] (E = Sb, Bi),¹¹ as evidenced by the similar percentage contributions to attractive interactions, with electrostatic being the most prominent. However, the magnitude of energy is significantly smaller here for both repulsive and attractive interactions (except for ΔE_{disp}) and the total interaction energy (ΔE_{int}) is also smaller (-109.4 (Sb), -111.2 (Bi) kcal/mol), presumably due to the diminished interactions of the arene platform in **2** versus those of the apical Sb or Bi elements.

The cleavage of the Cu–N coordination bonds during fragmentation means that the total ΔE_{int} does not directly indicate the interaction strengths between the crown-shaped Cu₃(μ₂-Cl)₃ and the rest of the complex. To address this issue, we divide the ΔE_{OrbInt} into pairwise interactions to provide a more detailed bonding picture between the fragments within the ETS-NOCV theoretical framework.²⁶ The ΔE_{OrbInt} contributions are denoted as $\Delta E_{\text{OrbInt},i}$ (i = integer) in order of energy strength. NOCV results show that there are no significant orbital interactions between the arene platform and the Cu₃(μ₂-Cl)₃ cluster; however, there are significant interactions associated with

the formation of the Cu–N coordination bond. NOCV pairs 1 - 3 have an energy of -37.58 kcal/mol associated with the Cu–N coordination bond with electrons flowing from both Cu and N contributing to the bond (Figure 5a), while the remaining NOCV pairs have an energy of less than 3 kcal/mol. Negligible electron flow is seen in the rest of the NOCV pairs from the copper atoms to the nitrogen atoms (Figure 5b). The independent gradient model based on the Hirshfeld partition (IGMH),²⁷ which analyzes noncovalent interactions, shows that there is a moderate interaction between the Cu₃ triangle and the π electrons of the arene platform. In Figure 5c/d, a green region is observed between the arene platform and Cu atoms, suggesting a pseudo η^2 binding mode between each copper and two arene carbon atoms with van der Waals interaction strength rather than that of traditional chemical bonds. The DFT calculations reveal that the Cu₃(μ_2 -Cl)₃ unit has an average Cu–Cl distance of 2.289 ± 0.004 Å, which is slightly shorter than that observed with apical Sb(III) and Bi(III) elements in lieu of the arene platform.¹¹ However, this is still longer than the average Cu–Cl distances of 2.166 ± 0.008 Å found in gas-phase Cu₃(μ_2 -Cl)₃ cluster (planar).¹⁷ The short distance may be due to a lack of trans influence²⁸ in comparison to that exerted by Sb/Bi.¹¹ The average Cu–Cu distance of 2.863 ± 0.038 Å (shorter than the experimental value) is also known in systems with cuprophilicity and is associated with a very low bond order.^{16,29} Overall, EDA and IGMH results suggest the major destabilization between Cu₃(μ_2 -Cl)₃ and the arene platform arises from three pairs of Cu–N coordination bonds, with negligible interactions between Cu atoms and π electrons of arene.

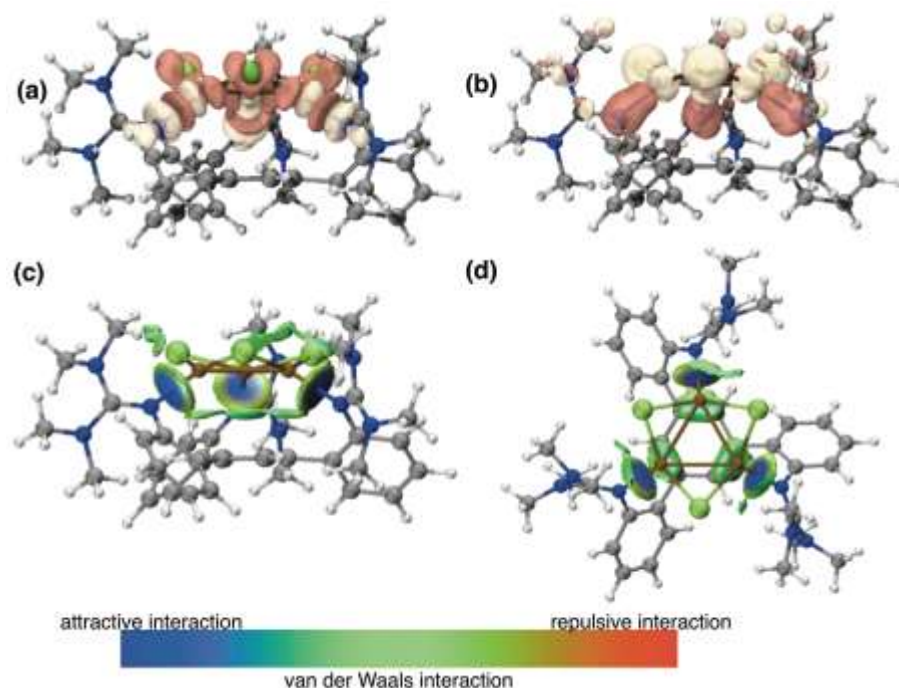


Figure 5. Deformation density maps (a) $\Delta E_{\text{OrbInt},1,2,3}$ (b) $\Delta E_{\text{OrbInt},\text{rest}}$ and Independent gradient model based on Hirshfeld partition (IGMH) (c) side view and (d) top view of **2**, respectively.

Table 1. Energy decomposition analysis (EDA) contributions of electrostatic attraction (ΔE_{elstat}), Pauli repulsion (ΔE_{Pauli}), orbital interaction (ΔE_{OrbInt}) and dispersion energy (ΔE_{disp}) to the total binding energy ΔE_{int} (energies in kcal/mol)

Model	ΔE_{elstat}	ΔE_{Pauli}	ΔE_{OrbInt}	ΔE_{disp}	ΔE_{int}
[(TMG ₃ trphen-Arene)Cu ₃ (μ-Cl) ₃] (2)	-172.7 (61.7%)	200.9	-80.0 (28.6%)	-27.0 (9.7%)	-78.8

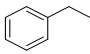
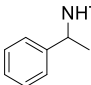
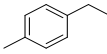
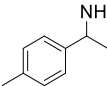
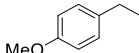
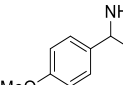
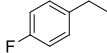
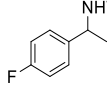
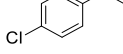
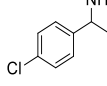
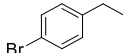
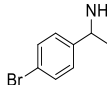
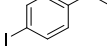
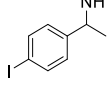
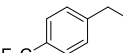
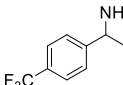
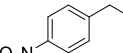
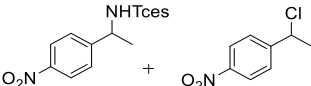
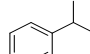
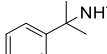
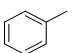
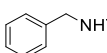
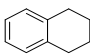
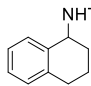
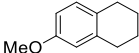
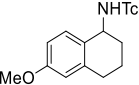
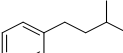
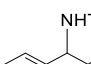
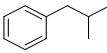
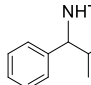
Catalytic C–H Amination Studies. A preliminary evaluation of the nitrene-transfer capabilities of [(TMG₃trphen-Arene)Cu₃(μ-Cl)₃] (**2**) was conducted with styrene (8 equiv.) and PhI=NTs (1 equiv.) in the presence of 5 mol% catalyst **2** and molecular sieves (5 Å) in CH₂Cl₂, to afford the corresponding aziridine in good yields (82%). The more challenging catalytic C–H amination of several substrates was subsequently pursued. Initial efforts to effect the catalytic amination of the benchmark substrate ethylbenzene (1 equiv.) by PhI=NTs (2 equiv.), mediated by **2** (5 mol %) in various solvents, afforded the benzylic amination product in less than 10% yield (Table S3). The more electrophilic PhI=NTces (Tces = 2,2,2-trichloroethoxysulfonyl) was then


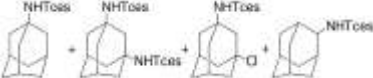




selected for further exploration and proved to be significantly more productive if delivered as pre-synthesized PhI=NTces ³⁰ (in lieu of being generated in situ from TcesNH_2 and $\text{PhI(O}_2\text{CR)}_2$ ($\text{R} = \text{Me, 'Bu}$). PhI=NTces has good solubility in many solvents (it can be crystallized from MeCN or acetone),³¹ but can be unstable in halogenated solvents. Among several solvent systems explored for the catalytic amination, chlorobenzene, α,α,α -trifluorotoluene and 1,2-difluorobenzene were most beneficial, especially in the presence of a small amount of HFIP (10% in volume, Table S3). $\text{PhCF}_3/\text{HFIP}$ (10:1 v/v) was selected for investigating the reaction scope, since PhINTces has prolonged stability in this solvent mixture (30 °C) in the absence of light. Attempts to aminate ethylbenzene with 2.5 or 10 mol% of catalyst, or in a substrate/ PhINTces ratio of 1:1 or 2:1, lead to lower yields (Table S3).

Table 2 summarizes product yields for the amination of several substrates (mostly benzylic) by employing the substrate as limiting reagent (1 equiv.) and PhI=NTces (2 equiv.) in the presence of **2** (5 mol%) and molecular sieves (5 Å), in $\text{PhCF}_3/\text{HFIP}$ (10:1 v/v). The catalytic reactions are allowed to run for 24 hours in a N_2 -filled dry box (30 °C). The products are purified on a silica column to remove the remaining substrate and catalyst components and quantified by ^1H NMR with the assistance of an internal standard. Good mass balances are obtained with respect to the substrate ($\geq 90\%$) and excess TcesNH_2 is observed in all cases. Under the optimum conditions, a panel of para-substituted ethylbenzenes (entries 1 - 9) provide the corresponding products of benzylic amination in modest to good yields. Ethylbenzene itself is aminated in a 42% yield, which drops to 18% if HFIP is not used. Higher yields ($\sim 50\%$) are obtained for electron-donating para-substituents (entries 2, 3), but also for halides F and Cl that tend to provide good resonance polar- and spin-delocalization effects, respectively.³² Other typical electron-withdrawing para-substituents (entries 8, 9) give very low yields, which in the case of p- NO_2 also include chlorinated

rather than aminated products. Primary and tertiary benzylic C–H bonds (entries 10, 11) afford amination products in low yields, presumably due to the high C–H bond energy³³ and steric protection, respectively. The electronic effect of a strong electron-donating substituent is also evident in the benzylic amination of 1,2,3,4-tetrahydronaphthalene and derivative (entries 12, 13). Competition between benzylic and tert-C–H bonds favor benzylic amination exclusively, but yields are low due to steric encumbrance (entries 14, 15). On the other hand, adamantane is functionalized in good overall yields (49%). Interestingly, the product profile (entry 16) includes three products of tert-C–H functionalization, with 1-Ad-NHTces being the major product (ORTEP for the disubstituted adamantanes, Figure S1; crystallographic data, Table S2), as well as a single, minor product of sec-C–H amination (2-Ad-NHTces). The mechanistically diagnostic *cis*- and *trans*-1,4-dimethylcyclohexane (entries 17, 18) provide moderate to low yields of *cis*- and *trans*-tert-C–H amination products (ORTEP, Figure S1; crystallographic data, Table S2), along with minor unidentified sec-amination products. Importantly, partial retention of stereochemistry is observed upon amination of the tert-C–H sites (*cis/trans* = 4.5 for *cis* substrate; *trans/cis* = 5.0 for *trans* substrate). Computational studies (BP86 functional) indicate that a *trans* conformer of the amination product is the most energetically stable, lying 1.4 kcal/mol underneath a low-energy *cis* conformer (Figure S2). The selectivity of **2** with this substrate lies between that of [Rh₂(esp)₂] (retention of stereochemistry)³⁴ and that of a bulky β -diketimato-Cu catalyst (complete erosion of stereochemistry).³⁵ These tert-C–H aminations also confirm that catalyst **2** is more effective than the Sb/Bi analogs (Figure 2).

Table 2. Yields of Catalytic Aminations of Substrates Mediated by [(TMG₃trphen-Arene)Cu₃(μ-Cl)₃] (**2**)

Entry No.	Substrate	Product	Yield (%)
1.			42
2.			47
3.			52
4.			53
5.			45
6.			27
7.			30
8.			12
9.			2, 10
10.			17
11.			14
12.			34
13.			49
14.			26
15.			21

16.			25, 14, 7, 3
17.			25 (<i>cis/trans</i> = 4.5)
18.			16 (<i>trans/cis</i> = 5.0)

^aConditions: Catalyst **2**, 0.0125 mmol (5 mol %); PhINTces, 0.50 mmol; substrate, 0.25 mmol; MS 5 Å, 20 mg; solvent (PhCF₃/HFIP 10:1 v/v), 0.500 g; 30 °C; 24 h.

Mechanistic Studies. (a) Hammett Plots. To gain insights in the mode of operation of catalyst **2**, Hammett plots were constructed for the competitive amination (PhI=NTces, 2 equiv.) of several p-X-ethylbenzenes (X = MeO, Me, F, Cl, Br, I, CF₃) versus ethylbenzene (1 equiv. each) catalyzed by **2** (5 mol%) in PhCF₃/HFIP (10:1 v/v) at 30 °C (6 h). Linear free-energy correlations of log (k_X/k_H) versus the polar substituent parameter σ_p can be obtained with satisfactory fit ($\rho_p = -1.22$, $R^2 = 0.93$), which can be further improved by employing the resonance-sensitive parameter σ^+ ($\rho^+ = -0.88$, $R^2 = 0.96$) (Figure 6 and Table S4). The negative ρ_p and ρ^+ coefficients suggest that significant positive charge develops at the benzylic carbon because of progressive C–H bond elongation en route to the transition state and eventual H-atom abstraction by an electrophilic amination entity. The ρ^+ value is less negative than that obtained for the Sb(III) analog [(TMG₃trphen-Sb)Cu₃(μ -Cl)₃] ($\rho^+ = -1.22$ (NTces))¹¹ and comparable to those evaluated in other copper-catalyzed aminations of benzylic substrates (ethylbenzene, toluene) in our lab by mononuclear Cu sites ($\rho^+ = -1.16$ (NTs), -0.91 (NNs), -0.89 (NTces)).^{8,31} These Cu- and analogous Ru-mediated ($\rho^+ = -0.90$, -1.49)³⁶ C–H aminations are perceived to operate via stepwise amination steps (H-atom abstraction, radical recombination). More modest negative ρ^+ values are obtained in *bona fide* concerted (asynchronous) amination mechanisms mediated by Rh reagents (-0.47 , -0.55 ,

-0.66, -0.73, -0.90).^{34,37-40} From this perspective, the activity of catalyst **2** is more consistent with stepwise operation but lies at the borderline with concerted paths.

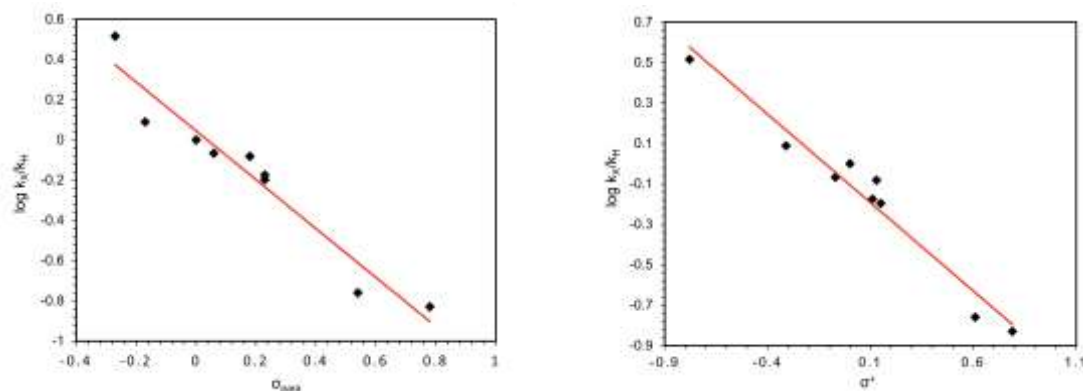
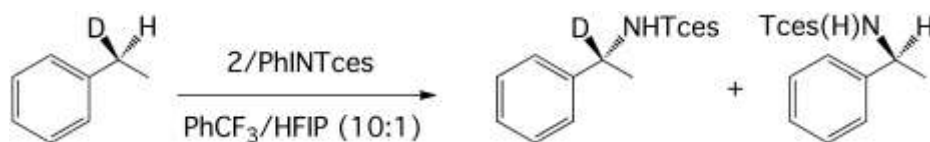


Figure 6. Linear free energy correlation of $\log(k_X/k_H)$ as a function of σ_p (left) ($\rho_p = -1.22$, $R^2 = 0.93$) and σ^+ (right) ($\rho^+ = -0.88$, $R^2 = 0.96$) for the competitive amination of para-substituted ethylbenzenes versus ethylbenzene catalyzed by [(TMG₃trphen-Arene)Cu₃(μ -Cl)₃] (**2**).

(b) Kinetic Isotope Effects (KIE). An experimental H(D) kinetic isotope effect was evaluated by means of a competitive H(D) amination (PhN=Tces, 1 equiv.) of the benzylic position of (*S*)-(+)-1-*d*-ethylbenzene ($D_1 \geq 99\%$, 1.5 equiv.) in the presence of catalyst **2** (5 mol%) in PhCF₃/HFIP (10: 1 v/v) under the conditions noted above. The substrate was prepared by a recently reported benzylic deuteration protocol⁴¹ that proceeds with excellent deuterium incorporation. The KIE value was determined from the H/D content of the benzylic position of the amination products (Scheme 3), as evaluated by ¹H NMR integration. The observed KIE value of $k_{H,d}/k_{D,h} = 2.1 \pm 0.1$ (lower case letters denote the spectator element) is a composite of primary and secondary effects for the abstraction of a hydrogen atom ($k_{obs} = (k_{H,h}/k_{D,h})_{prim}(k_{H,d}/k_{H,h})_{sec}$),⁴² therefore, the primary KIE value is most likely higher than the observed value (~ 2.4 for an average secondary KIE value of 1.15). Although the possibility of a turnover-limiting C–H bond activation step cannot be secured from these experiments, the KIE value obtained is on the low side of similar KIE values reported for intramolecular benzylic aminations (PhI=NTces) of PhC(H/D)(CH₂)₂OAc, such as

with catalysts $[\text{Mn}^{\text{III}}(\text{ClPc})](\text{SbF}_6)$ ($k_{\text{H}}/k_{\text{D}} = 3.00 \pm 0.08$ (intramolecular), 2.5 ± 0.2 (intermolecular)⁴³ and $[\text{Rh}_2(\text{esp})_2]$ ($k_{\text{H}}/k_{\text{D}} = 2.60 \pm 0.03$).³⁴ The Mn catalyst is reported to operate via a stepwise mechanism, whereas the Rh catalyst via concerted (asynchronous) activation of the benzylic C–H bond. The low primary KIE value observed with catalyst **2** may also be due to a bent transition-state structure, enforced by the narrow confinements in the accommodation of the active metal nitrene (*vide infra*).

Scheme 3. H(D) Competition Reaction in the Amination of (*S*)-(+)-1-*d*-ethylbenzene



Computational Cu₃-Nitrene Interaction Studies. To further specify the geometric and electronic properties of the active Cu=NR active species, copper nitrenes (for convenience, R = SO₂Ph) were optimized with the ORCA 4 program, using the TPSSh functional⁴⁴ with the def2-TZVP⁴⁵ basis set with auxiliary basis def2/J⁴⁶ and a dispersion correction that included Becke-Johnson damping.⁴⁷ The singlet, triplet and broken symmetry (BS) open-shell singlet (2,1) were each geometry optimized. Non-orthogonal magnetic orbitals of the broken symmetry solution show that a broken symmetry singlet solution exists.

The TPSSh/def2-TZVP level of theory is known to give accurate results with copper systems.⁴⁶ Equilibria may be assumed since the various states and configurations were close in energy. In all cases, the tricopper complexes feature a nitrene bridging two copper sites (Figures 7 (triplet) and S3 (singlet, BS singlet). Dicopper nitrenes are known to exist in solid state and liquid media.^{35,48}

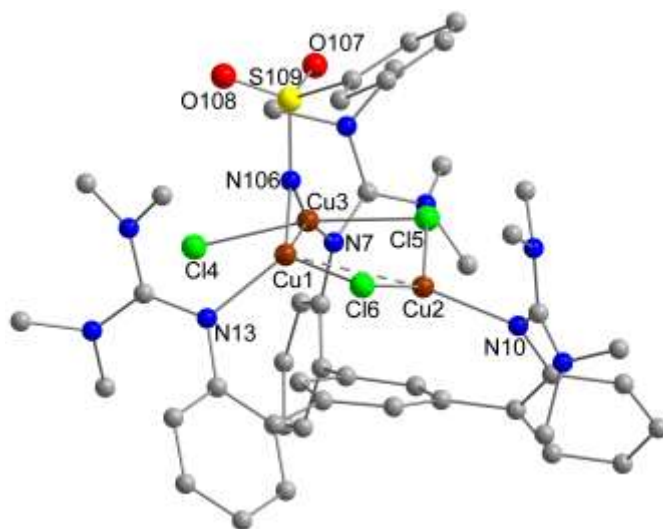


Figure 7. Optimized $[(\text{TMG}_3\text{trphen-Arene})\text{Cu}_3(\mu\text{-Cl})_3]$ with nitrene docked, optimized in a triplet $^3[\text{Cu}]\text{NR}$. Hydrogens are omitted from the figure for clarity. Selected bond lengths (\AA) and bond angles (deg): $\text{Cu}(1)\text{--N}(106) = 1.827$, $\text{Cu}(3)\text{--N}(106) = 1.937$, $\text{Cu}(1)\text{--Cu}(3) = 2.968$, $\text{Cu}(3)\text{--Cl}(4) = 2.293$, $\text{Cu}(1)\text{--N}(106)\text{--Cu}(3) = 104.06$, $\text{Cu}(3)\text{--N}(106)\text{--S}(109) = 118.98$, $\text{Cu}(1)\text{--N}(106)\text{--S}(109) = 136.78$, $\text{Cl}(4)\text{--Cu}(3)\text{--N}(106) = 93.24$.

The intact $[(\text{TMG})_3\text{trphen-Arene})\text{Cu}_3(\mu\text{-Cl})_3]$ (TPSSh optimized for direct comparison, Figure S4) has an average Mayer bond order of 0.179 for Cu–Cu, which is typical for complexes with cuprophilic interactions.¹⁶ However, a deviation from the C_3 symmetry of the $\text{Cu}_3(\mu\text{-Cl})_3$ is noticed with the nitrene-docked systems. The most stable calculated nitrene is the triplet state with the spin density distributed mostly on the nitrene's N and the two copper atoms that are bridged by the nitrene nitrogen. The spin population shows about +0.82 unpaired e^- on both copper atoms and approximately +0.60 e^- on the bridging nitrene nitrogen (Figure 8). The remaining spin density is localized on the neighboring Cl atom, which assumes a terminal rather than bridging coordination.

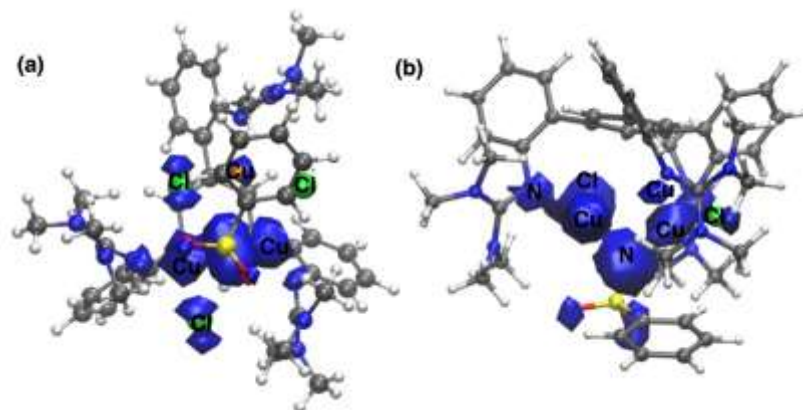


Figure 8. (a) Front and (b) side view of spin density profile for triplet state $^3[\text{Cu}]\text{NR}$ (TPSSh/def2-TZVP; Isovalue = 0.002). The blue surface indicates excess α -electron density.

As expected, the $^3[\text{Cu}]\text{NR}$ (Figure 7) features the shortest $\text{Cu}_2-(\mu\text{-NR})$ bonds in the complex with distances of 1.827 and 1.937 Å (the latter Cu carries the terminal Cl atom) and a Cu–Cu distance of 2.968 Å (Table 3), not unlike those reported previously for dicopper nitrenes.^{35,49} The Cu–N–R angles are 136.7 and 118.9° for the ligating copper atoms. The closed-shell singlet $^1[\text{Cu}]\text{NR}$ (Figure S3) is destabilized relative to the triplet ground state by 12.5 kcal/mol, while the broken symmetry open-shell singlet $^{\text{BS}}[\text{Cu}]\text{NR}$ (Figure S3) is only slightly destabilized by 1.0 kcal/mol versus the triplet (Table 4). The broken symmetry singlet solution has similar angles and distances to the ground state triplet (Table 3). For instance, the short Cu–NR bond distances at 1.826 and 1.941 Å are almost identical to those noted for $^3[\text{Cu}]\text{NR}$ (Table 3). One copper atom and bridging nitrene nitrogen have positive spin that sums to approximately 0.34 e^- , while the second copper atom and the terminal Cl carry the negative spin density summing to $\sim -0.32 e^-$ (Figure S5). The destabilized closed-shell singlet $^1[\text{Cu}]\text{NR}$ has Cu–NR distances at 2.013 and 1.989 Å, which are longer than the corresponding values for the ground-state triplet and broken-symmetry singlet solutions. The Cu–N–R values for both copper atoms are 126.5° and 113.1°.

Table 3. The coordination core of the optimized ¹[Cu]NR, ^{BS}[Cu]NR, and ³[Cu]NR showing selected bond length (Å) and bond angles (°) (R = SO₂Ph).

Bond length	¹ [Cu]NR	^{BS} [Cu]NR	³ [Cu]NR
Cu(3)–Cl(5)	2.272	2.391	2.396
Cu(3)–N(106)(NR)	2.012	1.941	1.937
Cu(3)–N(7)	2.127	1.990	1.994
Cu(1)–N(106)(NR)	1.990	1.826	1.827
Cu(3)–Cl(4)	3.271	2.297	2.293
Cu(1)–N(13)	2.113	1.965	1.968
Cu(1)–Cl(6)	2.312	2.277	2.277
Cu(2)–N(10)	2.146	2.078	2.080
Cu(2)–Cl(6)	2.281	2.352	2.350
Cu(2)–Cl(5)	2.278	2.273	2.267
Cu(1)–Cu(3)	2.751	2.962	2.968
Cu(1)–N(106)–Cu(3)	86.9	103.6	104.1
Cu(1)–N(106)–R	126.6	136.8	136.8
Cu(3)–N(106)–R	113.2	119.3	118.9

Table 4. Energy of the singlet, triplet, and broken symmetry relative to the triplet ground state

Spin State	kcal/mol (Tpssh/def2tzvp)
Singlet, ¹ [Cu]NR	12.5
Triplet, ³ [Cu]NR	0
Broken-symmetry singlet, ^{BS} [Cu]NR	1.0

Summary and Conclusions

The following are the major findings and insights garnered from the present investigation:

- (i) A new tripodal ligand has been constructed featuring a benzene platform and phenylene arms decorated with superbasic tetramethylguanidinyll arms residing on the same side of the benzene ring. This pre-organized ligand framework extracts a $\text{Cu}_3(\mu_2\text{-Cl})_3$ cluster from anhydrous CuCl , to generate a compound with $(\text{TMG}_3\text{trphen-Arene})\text{Cu}_3(\mu\text{-Cl})_3$ stoichiometry. Single-crystal X-ray structural analysis reveals that a crown-shaped $\text{Cu}_3(\mu_2\text{-Cl})_3$ unit is supported by three guanidinyll moieties, each coordinated to a single Cu(I) site, and via long-distant contacts with the benzene platform. Both left- and right-hand propeller conformations are noted in the unit cell of the compound. A relaxed version of this structure is retained in solution, featuring equivalent phenylene and TMG moieties on the NMR timescale.
- (ii) Energy decomposition analysis (EDA) applied to $[(\text{TMG}_3\text{trphen-Arene})\text{Cu}_3(\mu\text{-Cl})_3]$ (2) suggests that the electrostatic component (62%) is a dominant contributor among attractive interactions, followed by orbital interactions (28%) and dispersion energy (10%) contributions. The natural orbitals for chemical valence (NOCV) analysis indicate that the dominant orbital interactions are associated with the $\text{Cu(I)}\text{-N}_{\text{TMG}}$ bonds. Very little, if any, orbital engagement is observed between the Cu_3 triangle and the benzene platform. Nevertheless, the independent gradient model based on Hirshfeld partition (IGMH) method supports weak noncovalent interactions of the $\text{Cu}/\eta^2\text{-benzene}$ type, as well as long-range cuprophilic contacts.
- (iii) An initial evaluation of catalytic C–H aminations mediated by $[(\text{TMG}_3\text{trphen-Arene})\text{Cu}_3(\mu\text{-Cl})_3]$ demonstrates that common electrophilic N-donor partners (such as NTs) are rather

unproductive. The more electrophilic nitrene source $\text{PhI}=\text{NTces}$ provides modest to good yields for the C–H amination of a panel of benzylic substrates, especially in the presence of low amounts of HFIP in the solvent matrix ($\text{PhCF}_3/\text{HFIP}$, 10:1 v/v). Electron-rich benzylic substrates are naturally more reactive than electron-deficient congeners, and steric encumbrance is usually detrimental. Tert-C–H bonds are also undergoing amination, with partial retention of stereochemistry for the diagnostic *cis*- and *trans*-1,4-dimethylcyclohexane.

- (iv) Hammett plots for the competitive p-X-ethylbenzene/ethylbenzene amination (PhINTces) mediated by catalyst **2**, provide small negative ρ_p and ρ^+ coefficients. An intramolecular competition for the amination of the benzylic C–H(D) site of monodeuterated ethylbenzene furnish rather modest primary KIE values. The observed Hammett parameters and KIE values lie at the borderline with respect to analogous values reported for concerted (asynchronous) and stepwise (H-atom abstraction/radical recombination) C–H aminations pathways.
- (v) Computational (DFT) exploration of nitrene docking to the Cu_3 cluster suggests that the nitrene is bridging via the N atom between two copper sites with concomitant relocation of the bridging chloride to a terminal position, giving rise to a triplet ground state and a closely spaced broken-symmetry singlet state. The small energy difference indicates that both states may contribute to the observed reactivity in agreement with the borderline mechanistic indicators noted above.

Future studies will address chlorinated-free versions of the present reagent and explore C–H bond aminations with a wider range of C–H substrates. Moreover, the mechanistic intricacies unraveled in the present study will be further investigated with an arsenal of diagnostic probes and computational assistance.

Author contributions

The manuscript was written through contributions of all authors. All authors have approved the final version of the manuscript.

Conflicts of interest

There are no conflicts to declare.

Acknowledgements

The authors (P.S.) are grateful for the generous funding awarded by NIH/NIGMS (R15GM117508 and R15GM139071) for this work. Drs. Steven Kelley and Shaokai Jiang are acknowledged for collecting single-crystal X-ray diffraction and NMR data at the University of Missouri-Columbia, respectively. T.R.C. acknowledges partial support of this research through grant DE-FG02-03ER15387 from the U.S. Department of Energy, Basic Sciences, Catalysis Science program.

Notes and references**Accession Codes**

CCDC 2345650, 2345651, 2361010, 2361011, 2361012, and 2361013 contain the supplementary crystallographic data for this paper. These data can be obtained free of charge via www.ccdc.cam.ac.uk/data_request/cif, or by emailing data_request@ccdc.cam.ac.uk, or by contacting The Cambridge Crystallographic Data Centre, 12 Union Road, Cambridge CB2 1EZ, UK; fax: +44 1223 336033.

References

- (1) Eller, K.; Henkes, E.; Rossbacher, R.; Höke, H. *Amines, Aliphatic*; Ullmann's Encyclopedia of Industrial Chemistry. Weinheim: Wiley-VCH, 2005.
- (2) (a) Hartwig, J. F.; Kawatsura, M.; Hauck, S. I.; Shaughnessy, K. H.; Alcazar-Roman, L. M. Room-Temperature Palladium-Catalyzed Amination of Aryl Bromides and Chlorides and Extended Scope of Aromatic C–N Bond Formation with a Commercial Ligand. *J. Org. Chem.* **1999**, *64*, 5575-5580. (b) Wolfe, J. P.; Buchwald, S. L. Scope and Limitations of the Pd/BINAP-Catalyzed Amination of Aryl Bromides. *J. Org. Chem.* **2000**, *65*, 1144-1157. (c) Lam, P. Y. S.; Clark, C. G.; Saubern, S.; Adams, J.; Winters, M. P.; Chan, D. M. T.; Combs, A. New aryl/heteroaryl C–N bond cross-coupling reactions via arylboronic acid/cupric acetate arylation. *Tetrahedron Lett.* **1998**, *39*, 2941-2944. (d) Rao, K. S.; Wu, T.-S. Chan-Lam coupling reactions: synthesis of heterocycles. *Tetrahedron* **2012**, *68*, 7735-7754.
- (3) (a) Park, Y., Kim, Y.; Chang, S. Transition Metal-Catalyzed C–H Amination: Scope, Mechanism, and Applications. *Chem. Rev.* **2017**, *117*, 9247-9301. (b) Roizen, J. L.; Harvey, M. E.; Du Bois, J. Metal-Catalyzed Nitrogen-Atom Transfer Methods for the Oxidation of Aliphatic C–H Bonds. *Acc. Chem. Res.* **2012**, *45*, 911-922. (c) Ju, M.; Schomaker, J. M. Nitrene Transfer Catalysts for Enantioselective C–N Bond Formation. *Nat. Rev. Chem.* **2021**, *5*, 580-594. (d) Chandrachud, P. P.; Jenkins, D. M. Transition Metal Aziridination Catalysts, in *Encyclopedia of Inorganic and Bioinorganic Chemistry*; Wiley Online Library, 2017; pp. 1-11.
- (4) (a) Collet, F.; Lescot, C.; Dauban, P. Catalytic C–H amination: the stereoselectivity issue. *Chem. Soc. Rev.* **2011**, *40*, 1926-1936. (b) Dequierez, G.; Pons, V.; Dauban, P. Nitrene Chemistry in Organic Synthesis: Still in Its Infancy? *Angew. Chem. Int. Ed.* **2012**, *51*, 7384-

7395. (c) Hazelard, D.; Nocquet, P.-A.; Compain, P. Catalytic C–H amination at its limits: challenges and solutions. *Org. Chem. Front.* **2017**, *4*, 2500-2521.
- (5) Noda, H.; Tang, X.; Shibasaki, M. Catalyst-Controlled Chemoselective Nitrene Transfers. *Helv. Chim. Acta* **2021**, *104*, e2100140.
- (6) (a) Barbolla, I.; Sotomayor, N.; Lete, E. Transition metal-guanidine complexes as catalysts in organic reactions. Recent developments. *Arkivoc* **2020**, *vii*, 158-179. (b) Cui, X.-Y.; Tan, C.-H.; Leow, D. Metal-catalysed reactions enabled by guanidine-type ligands. *Org. Biomol. Chem.* **2019**, *17*, 4689-4699.
- (7) (a) Malik, D. D.; Chandra, A.; Seo, M. S.; Lee, Y.-M.; Farquhar, E. R.; Mebs, S.; Dau, H.; Ray, K.; Nam, W. Formation of cobalt-oxygen intermediates by dioxygen activation at a mononuclear nonheme cobalt(II) center. *Dalton Trans.* **2021**, *50*, 11889-11898. (b) Comba, P.; Löhr, A.-M.; Pfaff, F.; Ray, K. Redox Potentials of High-Valent Iron-, Cobalt-, and Nickel-Oxido Complexes: Evidence for Exchange Enhanced Reactivity. *Isr. J. Chem.* **2020**, *60*, 957-962. (c) Liu, J. J.; Siegler, M. A.; Karlin, K. D.; Moënne-Loccoz, P. Direct Resonance Raman Characterization of a Peroxynitrito Copper Complex Generated from O₂ and NO and Mechanistic Insights into Metal-Mediated Peroxynitrite Decomposition. *Angew. Chem. Int. Ed.* **2019**, *58*, 10936-10940. (d) Speelman, A. L.; White, C. J.; Zhang, B.; Alp, E. E.; Zhao, J.; Hu, M.; Krebs, C.; Penner-Hahn, J.; Lehnert, N. Non-heme High-Spin {FeNO}⁶⁻⁸ Complexes: One Ligand Platform Can Do it All. *J. Am. Chem. Soc.* **2018**, *140*, 11341-11359. (e) England, J.; Guo, Y.; Van Heuvelen, K. M.; Cranswick, M. A.; Rohde, G. T.; Bominaar, E. L.; Münck, E.; Que, L., Jr. A More Reactive Trigonal-Bipyramidal High-Spin Oxoiron(IV) Complex with a cis-Labile Site. *J. Am. Chem. Soc.* **2011**, *133*, 11880-11883.

- (8) Bagchi, V.; Paraskevopoulou, P.; Das, P.; Chi, L.; Wang, Q.; Choudhury, A.; Mathieson, J. S.; Cronin, L.; Pardue, D. B.; Cundari, T. R.; Mitrikas, G.; Sanakis, Y.; Stavropoulos, P. A versatile Tripodal Cu(I) Reagent for C–N Bond Construction via Nitrene-Transfer Chemistry: Catalytic Perspectives and Mechanistic Insights on C–H Aminations/Amidinations and Olefin Aziridinations. *J. Am. Chem. Soc.* **2014**, *136*, 11362-11381.
- (9) Sahoo, S. K.; Harfmann, B.; Ai, L.; Wang, Q.; Mohapatra, S.; Choudhury, A.; Stavropoulos, P. Cationic Divalent Metal Sites (M = Mn, Fe, Co) Operating as Both Nitrene-Transfer Agents and Lewis Acids toward Mediating the Synthesis of Three- and Five-Membered *N*-Heterocycles. *Inorg. Chem.* **2023**, *62*, 10743-10761.
- (10) (a) Bernasconi, L.; Louwerse, M. J.; Baerends, E. J. The Role of Equatorial and Axial Ligands in Promoting the Activity of Non-Heme Oxidoiron(IV) Catalysts in Alkane Hydroxylation. *Eur. J. Inorg. Chem.* **2007**, 3023-3033. (b) Hirao, H.; Que, L., Jr.; Nam, W.; Shaik, S. A Two-State Reactivity Rationale for Counterintuitive Axial Ligand Effects on the C–H Activation Reactivity of Nonheme Fe^{IV}=O Oxidants. *Chem. Eur. J.* **2008**, *14*, 1740-1756. (c) Collins, L. R.; van Gastel, M.; Neese, F.; Fürstner, A. Enhanced Electrophilicity of Heterobimetallic Bi–Rh Paddlewheel Carbene Complexes: A Combined Experimental, Spectroscopic, and Computational Study. *J. Am. Chem. Soc.* **2018**, *140*, 13042-13055.
- (11) Sharma, M.; Fritz, R. M.; Adebajo, J. O.; Lu, Z.; Cundari, T. R.; Omary, M. A.; Choudhury, A.; Stavropoulos, P. Nitrene-Transfer Chemistry to C–H and C=C Bonds Mediated by Triangular Coinage Metal Platforms Supported by Triply Bridging Pnictogen Elements Sb(III) and Bi(III). *Organometallics* **2024**, *43*, 634-652.

- (12) (a) Hillenbrand, J.; Leutzsch, M.; Yiannakas, E.; Gordon, C. P.; Wille, C.; Nöthling, N.; Copéret, C.; Fürstner, A. "Canopy Catalysts" for Alkyne Metathesis: Molybdenum Alkylidyne Complexes with a Tripodal Ligand Framework. *J. Am. Chem. Soc.* **2020**, *142*, 11279–11294. (b) Cook, B. J.; Di Francesco, G. N.; Kieber-Emmons, M. T.; Murray, L. J. A Tricopper(I) Complex Competent for O Atom Transfer, C–H Bond Activation, and Multiple O₂ Activation Steps. *Inorg. Chem.* **2018**, *57*, 11361–11368. (c) Murray, L. J.; Weare, W. W.; Shearer, J.; Mitchell, A. D.; Abboud, K. A. Isolation of a (Dinitrogen)Tricopper(I) Complex. *J. Am. Chem. Soc.* **2014**, *136*, 13502–13505. (d) Hu, X.; Meyer, K. New tripodal N-heterocyclic carbene chelators for small molecule activation. *J. Organomet. Chem.* **2005**, *690*, 5474–5484. (e) Liu, H.-K.; Sun, W.-Y.; Tang, W.-X.; Tan, X.-Y.; Zhang, H.-X.; Tong, Y.-X.; Yu, X.-L.; Kang, B.-S. Assembly of supramolecular complexes with tripodal ligand titmb and tib: a 2D rhombic grid network assembled from 2-connected tib. *J. Chem. Soc. Dalton Trans.* **2002**, 3886–3891. (f) Ohi, H.; Tachi, Y.; Itoh, S. Supramolecular and Coordination Polymer Complexes Supported by a Tripodal Tripyridine Ligand Containing a 1,3,5-Triethylbenzene Spacer. *Inorg. Chem.* **2004**, *43*, 4561–4563. (g) Wu, G.; Wang, X.-F.; Okamura, T.; Sun, W.-Y.; Ueyama, N. Syntheses, Structures, and Photoluminescence Properties of Metal(II) Halide Complexes with Pyridine-Containing Flexible Tripodal Ligands. *Inorg. Chem.* **2006**, *45*, 8523–8532. (h) Fan, J.; Sun, W.-Y.; Okamura, T.; Tang, W.-X.; Ueyama, N. *Inorg. Chem.* **2003**, *42*, 3168–3175.
- (13) (a) Piątek, P.; Słomiany, N. 1,3,5-Tris(2'-aminophenyl)benzene: A Novel Platform for Molecular Receptors. *Synlett* **2006**, 2027–2030. (b) Baudoin, O.; Guénard, D.; Guéritte, F. Palladium-Catalyzed Borylation of Ortho-Substituted Phenyl Halides and Application to the One-Pot Synthesis of 2,2'-Disubstituted Biphenyls. *J. Org. Chem.* **2000**, *65*, 9268–9271.

- (14) Lan, Y.; Morimoto, Y.; Shimizu, I.; Sugimoto, H.; Itoh, S. Characterization and Reactivity Studies of Mononuclear Tetrahedral Copper(II)–Halide Complexes. *Inorg. Chem.* **2023**, *62*, 10539-10547.
- (15) Ke, I.-S.; Gabbaï, F. P. $\text{Cu}_3(\mu_2\text{-Cl})_3$ and $\text{Ag}_3(\mu_2\text{-Cl})_3$ Complexes Supported by Tetradentate Trisphosphino-stibine and -bismuthine Ligands: Structural Evidence for Triply Bridging Heavy Pnictines. *Aust. J. Chem.* **2013**, *66*, 1281-1287.
- (16) Baranov, A. Y.; Pritchina, E. A.; Berezin, A. S.; Samsonenko, D. G.; Fedin, V. P.; Belogorlova, N. A.; Gritsan, N. P.; Artem'ev, A. V. Beyond Classical Coordination Chemistry: The First Case of a Triply Bridging Phosphine Ligand. *Angew. Chem. Int. Ed.* **2021**, *60*, 12577-12584.
- (17) Hargittai, M.; Schwerdtfeger, P.; Réffy, B.; Brown, R. The Molecular Structure of Different Species of Cuprous Chloride from Gas-Phase Electron Diffraction and Quantum Chemical Calculations. *Chem. Eur. J.* **2003**, *9*, 327-333.
- (18) García-Romero, Á.; Waters, J. E.; Jethwa, R. B.; Bond, A. D.; Colebatch, A. L.; García-Rodríguez, R.; Wright, D. S. Highly Adaptive Nature of Group 15 *Tris*(quinolyl) Ligands—Studies with Coinage Metals. *Inorg. Chem.* **2023**, *62*, 4625-4636.
- (19) (a) Ito, H.; Abe, T.; Saigo, K. Enantioseparation and Electronic Properties of a Propeller-Shaped Triarylborane. *Angew. Chem. Int. Ed.* **2011**, *50*, 7144–7147. (b) Kemper, M.; Engelage, E.; Merten, C. Chiral Molecular Propellers of Triarylborane Ammonia Adducts. *Angew. Chem. Int. Ed.* **2021**, *60*, 2958–2962. (c) Kemper, M.; Reese, S.; Engelage, E.; Merten, C. Inducing Propeller Chirality in Triaryl Boranes with Chiral Amines. *Chem. Eur. J.* **2022**, *28*, e202202812.

- (20) Alvarez, S. A cartography of the van der Waals territories. *Dalton Trans.* **2013**, 42, 8617-8636.
- (21) (a) Zhang, L.; Li, X.-X.; Lang, Z.-L.; Liu, Y.; Liu, J.; Yuan, L.; Lu, W.-Y.; Xia, Y.-S.; Dong, L.-Z.; Yuan, D.-Q.; Lan, Y.-Q. Enhanced Cuprophilic Interactions in Crystalline Catalysts Facilitate the Highly Selective Electroreduction of CO₂ to CH₄. *J. Am. Chem. Soc.* **2021**, 143, 3808-3816. (b) Harisomayajula, N. V. S.; Makovetskyi, S.; Tsai, Y.-C. Cuprophilic Interactions in and between Molecular Entities. *Chem. Eur. J.* **2019**, 25, 8936-8954.
- (22) Raab, V.; Harms, K.; Sundermeyer, J.; Kovačević, B.; Maksić, Z. B. 1,8-Bis(dimethylethyleneguanidino)naphthalene: Tailoring the Basicity of Bisguanidine “Proton Sponges” by Experiment and Theory. *J. Org. Chem.* **2003**, 68, 8790-8797.
- (23) (a) Wright, A. M.; Irving, B. J.; Wu, G.; Meijer, A. J.; Hayton, T. W. A Copper(I)–Arene Complex with an Unsupported η^6 Interaction. *Angew. Chem. Int. Ed.* **2015**, 54, 3088–3091. (b) Parvin, N.; Hossain, J.; George, A.; Parameswaran, P.; Khan, S. N-heterocyclic silylene stabilized monocordinated copper(I)–arene cationic complexes and their application in click chemistry. *Chem. Commun.* **2020**, 56, 273–276. (c) Dattelbaum, A. M.; Martin, J. D. Benzene-Copper(I) Coordination in a Bimetallic Chain Complex. *Inorg. Chem.* **1999**, 38, 6200–6205. (d) Dargel, T. K.; Hertwig, R. H.; Koch, W. How do coinage metal ions bind to benzene? *Mol. Phys.* **1999**, 96, 583-591.
- (24) (a) Osako, T.; Tachi, Y.; Doe, M.; Shiro, M.; Ohkubo, K.; Fukuzumi, S.; Itoh, S. Quantitative Evaluation of d– π Interaction in Copper (I) Complexes and Control of Copper (I) Dioxygen Reactivity. *Chem. Eur. J.* **2004**, 10, 237–246. (b) Xu, F.-B.; Li, Q.-S.; Wu, L.-Z.; Leng, X.-B.; Li, Z.-C.; Zeng, X.-S.; Chow, Y. L.; Zhang, Z.-Z. Formation of Group 11 Metal(I)-Arene Complexes: Bonding Mode and Molecule-Responsive Spectral Variations. *Organometallics*

- 2003**, 22, 633-640. (c) Pérez-Galán, P.; Delpont, N.; Herrero-Gómez, E.; Maseras, F.; Echavarren, A. M. Metal–Arene Interactions in Dialkylbiarylphosphane Complexes of Copper, Silver, and Gold. *Chem. Eur. J.* **2010**, 16, 5324–5332.
- (25) Mascal, M.; Kerdelhué, J.; Blake, A. J.; Cooke, P. A. S-Cylindrophanes: From Metal Tweezers to Metal Sandwiches. *Angew. Chem. Int. Ed.* **1999**, 38, 1968–1970.
- (26) (a) Mitoraj, M. P.; Michalak, A.; Ziegler, T. A Combined Charge and Energy Decomposition Scheme for Bond Analysis. *J. Chem. Theory Comput.* **2009**, 5, 962–975. (b) Ziegler, T.; Rauk, A. Carbon Monoxide, Carbon Monosulfide, Molecular Nitrogen, Phosphorus Trifluoride, and Methyl Isocyanide as σ Donors and π Acceptors. A Theoretical Study by the Hartree-Fock-Slater Transition-State Method. *Inorg. Chem.* **1979**, 18, 1755–1759. (c) Ziegler, T.; Rauk, A. A Theoretical Study of the Ethylene-Metal Bond in Complexes between Cu^+ , Ag^+ , Au^+ , Pt^0 or Pt^{2+} and Ethylene, Based on the Hartree-Fock-Slater Transition-State Method. *Inorg. Chem.* **1979**, 18, 1558–1565.
- (27) Lu, T.; Chen, Q. Independent gradient model based on Hirshfeld partition: A new method for visual study of interactions in chemical systems. *J. Comput. Chem.* **2022**, 43, 539–555.
- (28) Anderson, K. M.; Orpen, A. G. On the relative magnitudes of *cis* and *trans* influences in metal complexes. *Chem. Commun.* **2001**, 2682-2683.
- (29) Mehrotra, P. K.; Hoffmann, R. Cu(I)–Cu(I) Interactions. Bonding Relationships in d^{10} - d^{10} Systems. *Inorg. Chem.* **1978**, 17, 2187-2189.
- (30) Van Leest, N. P.; Grooten, L.; van der Vlugt, J. I.; de Bruin, B. Uncatalyzed Oxidative C–H Amination of 9,10-Dihydro-9-Heteroanthracenes: A Mechanistic Study. *Chem. Eur. J.* **2019**, 25, 5987-5993.

- (31) Sahoo, S. K.; Harfmann, B.; Bhatia, H.; Singh, H.; Balijapelly, S.; Choudhury, A.; Stavropoulos, P. A Comparative Study of Cationic Copper(I) Reagents Supported by Bipodal Tetramethylguanidinyll-Containing Ligands as Nitrene-Transfer Catalysts. *ACS Omega* **2024**, *9*, 15697-15708.
- (32) Jiang, X.-K. Establishment and Successful Application of the σ_{J} Scale of Spin-Delocalization Substituent Constants. *Acc. Chem. Res.* **1997**, *30*, 283-289.
- (33) Nam, P.-C.; Nguyen, M. T.; Chandra, A. K. The C–H and α (C–X) Bond Dissociation Enthalpies of Toluene, C₆H₅–CH₂X (X = F, Cl), and Their Substituted Derivatives: A DFT Study. *J. Phys. Chem. A* **2005**, *109*, 10342-10347.
- (34) Fiori, K. W.; Du Bois, J. Catalytic Intermolecular Amination of C–H Bonds: Method Development and Mechanistic Insights. *J. Am. Chem. Soc.* **2007**, *129*, 562-568.
- (35) (a) Aguila, M. J. B.; Badiei, Y. M.; Warren, T. H. Mechanistic Insights into C–H Amination via Dicopper Nitrenes. *J. Am. Chem. Soc.* **2013**, *135*, 9399-9406. (b) Badiei, Y. M.; Dinescu, A.; Dai, X.; Palomino, R. M.; Heinemann, F. W.; Cundari, T. R.; Warren, T. H. *Angew. Chem. Int. Ed.* **2008**, *47*, 9961-9964. (c) Badiei, Y. M.; Krishnaswamy, A.; Melzer, M. M.; Warren, T. H. Transient Terminal Cu–Nitrene Intermediates from Discrete Dicopper Nitrenes. *J. Am. Chem. Soc.* **2006**, *128*, 15056-15057.
- (36) Harvey, M. E.; Musaev, D.; Du Bois, J. A Diruthenium Catalyst for Selective, Intramolecular Allylic C–H Amination: Reaction Development and Mechanistic Insight Gained through Experiment and Theory. *J. Am. Chem. Soc.* **2011**, *133*, 17207-17216.
- (37) Huard, K.; Lebel, H. N-Tosyloxycarbamates as Reagents in Rhodium-Catalyzed C–H Amination Reactions. *Chem. Eur. J.* **2008**, *14*, 6222-6230.

- (38) Fiori, K. W.; Espino, C. G.; Brodsky, B. H.; Du Bois, J. A mechanistic analysis of the Rh-catalyzed intramolecular C–H amination reaction. *Tetrahedron* **2009**, *65*, 3042-3051.
- (39) Park, S. H.; Kwak, J.; Shin, K.; Ryu, J.; Park, Y.; Chang, S. Mechanistic Studies of the Rhodium-Catalyzed Direct C–H Amination Reaction Using Azides as the Nitrogen Source. *J. Am. Chem. Soc.* **2014**, *136*, 2492-2502.
- (40) Nägeli, I.; Baud, C.; Bernardinelli, G.; Jacquier, Y.; Moran, M.; Müller, P. Rhodium(II)-Catalyzed CH Insertions with {[(4-Nitrophenyl)-sulfonyl]imino}phenyl- λ^3 -iodane. *Helv. Chim. Acta* **1997**, *80*, 1087-1105.
- (41) Mills, M. D.; Sonstrom, R. E.; Vang, Z. P.; Neill, J. L.; Scolati, H. N.; West, C. T.; Pate, B. H. Clark, J. R. Enantioselective Synthesis of Enantioisotopomers with Quantitative Chiral Analysis by Chiral Tag Rotational Spectroscopy. *Angew. Chem. Int. Ed.* **2022**, *61*, e202207275.
- (42) Muchalski, H.; Levonyak, A. J.; Xu, L.; Ingold, K. U.; Porter, N. A. Competition H(D) Kinetic Isotope Effects in the Autoxidation of Hydrocarbons. *J. Am. Chem. Soc.* **2015**, *137*, 94-97.
- (43) Clark, J. R.; Feng, K.; Sookezian, A.; White, M. C. Manganese-catalysed benzylic C(sp^3)–H amination for late-stage functionalization. *Nat. Chem.* **2018**, *10*, 583-591.
- (44) Staroverov, V. N.; Scuseria, G. E.; Tao, J.; Perdew, J. P. Comparative Assessment of a New Nonempirical Density Functional: Molecules and Hydrogen-Bonded Complexes. *J. Chem. Phys.* **2003**, *119*, 12129-12137.
- (45) Weigend, F.; Ahlrichs, R. Balanced Basis Sets of Split Valence, Triple Zeta Valence and Quadruple Zeta Valence Quality for H to Rn: Design and Assessment of Accuracy. *Phys. Chem. Chem. Phys.* **2005**, *7*, 3297-3305.

- (46) Weigend, F. Accurate Coulomb-Fitting Basis Sets for H to Rn. *Phys. Chem. Chem. Phys.* **2006**, 8, 1057-1065.
- (47) Grimme, S.; Ehrlich, S.; Goerigk, L. Effect of the Damping Function in Dispersion Corrected Density Functional Theory. *J. Comput. Chem.* **2011**, 32, 1456-1465.
- (48) Moegling, J.; Hoffmann, A.; Thomas, F.; Orth, N.; Liebhäuser, P.; Herber, U.; Rampmaier, R.; Stanek, J.; Fink, G.; Ivanović-Burmazović, I.; Herres-Pawlis, S. Designed To React: Terminal Copper Nitrenes and Their Application in Catalytic C–H Aminations. *Angew. Chem. Int. Ed.* **2018**, 57, 9154-9159.
- (49) Dielmann, F.; Andrada, D. M.; Frenking, G.; Bertrand, G. Isolation of Bridging and Terminal Coinage Metal–Nitrene Complexes. *J. Am. Chem. Soc.* **2014**, 136, 3800-3802.

Data for this article are available as Electronic Supplementary Information (ESI) upon publication of the article and include: synthetic protocols, NMR spectra, X-ray crystallography data and cif files deposited with accession numbers CCDC 2345650, 2345651, 2361010, 2361011, 2361012, and 2361013 (available at www.ccdc.cam.ac.uk/data_request/cif), computational xyz files, as well as additional computational details, figures and tables as noted in the text.